

# Intelligent Autonomous User Discovery and Link Maintenance for mmWave and TeraHertz Devices With Directional Antennas

Zaheer Khan<sup>✉</sup>, Janne J. Lehtomäki<sup>✉</sup>, *Member, IEEE*, Valerio Selis<sup>✉</sup>, Hamed Ahmadi<sup>✉</sup>,  
and Alan Marshall<sup>✉</sup>, *Senior Member, IEEE*

**Abstract**—Use of smart directional antennas in handheld devices to generate a narrow beam in different directions for mmWave/TeraHertz communications present significant challenges. Devices using such antennas may have to scan several different directions in three-dimensional (3D) space to discover another user or an access point, a process that can result in problematic delays. Moreover, small movements of a user/device in the form of rotation and/or displacement may cause the discovered link to be lost. This paper proposes adaptive link discovery algorithms for devices in both infrastructure/ad hoc networks and evaluates their performance in terms of time-to-discovery. We show that one of the two proposed methods provides guaranteed discovery. We use an inertial measurement unit sensor to help intelligently rediscover a lost/degraded link. We propose sensor assisted link prediction methods for low-latency rediscovery in 3D space. We evaluate the effectiveness of our prediction-based rediscovery methods by testing them with real datasets representing various user/device 3D rotation patterns. We show that the smoothing based rediscovery can reach the prediction accuracy to 100% when two antenna sectors are searched, and it reduces the time-to-rediscovery by up to  $Sx$  ( $S$  times) as compared to the time-to-discovery, where  $S$  is the number of antenna sectors.

**Index Terms**—5G, teraHertz, mmWave, directional antenna, IMU sensor, orientation, and predictions, 6G.

## I. INTRODUCTION

**T**O ENABLE the sixth generation (6G) wireless networks and to support a wide range of services, improved spectral efficiency in existing spectrum bands and efficient access to new spectrum bands will be fundamental [1]. The mmWave frequency spectrum is one of the promising candidate bands

for both 5G backhaul and radio access as it offers the availability of huge bandwidths [2]. For beyond 5G systems, teraHertz wireless communication has also been proposed. For example, world radio conference (WRC) 2019 has considered the use of frequency band 275–450 GHz for communication. Free space path loss (and potentially molecular absorption) dramatically increases in mmWave and teraHertz frequency spectrum and to enable wireless communication highly directional antennas are needed in both uplink and downlink of wireless systems operating in these bands [3], [4]. Highly directional antennas are often called “pencil beam” antennas.

For short-range communication scenarios in future wireless networks, visible light communication (VLC) technology is a favorable complementary wireless communication technology to mmWave communications. Highly directional VLC light beams can be generated using light-emitting diodes which act as antennas and communicate data to users via modulating light intensity [5]. Free-space optical (FSO) communications is another highly directional line-of-sight technology that has attracted considerable interest for future networks as it has the potential to provide transmissions at very high data rates between two terminals. It also employs narrow and directional modulated light beams and requires beam acquisition and beam direction pointing mechanisms to operate efficiently [6].

New algorithms are necessary that allow users to efficiently perform both initial link discovery and also subsequent link rediscovery/maintenance using directional antennas. This is due to the reason that focusing energy in one particular direction creates challenges in terms of user discovery as when two users use a directional antenna they may discover each other only if they direct the beam toward each other at the same time. Moreover, changes in orientation due to rotation and/or displacement may result in the loss/degradation of an already established communication link and may require some link rediscovery/maintenance mechanism. *Intelligent ways* to track or keep some estimates of spatial directions such as those proposed in this paper can help to communicate with less signaling overhead.

Wireless devices, such as smartphones and tablets, contain various embedded sensors. This has made it possible to use their assistance in the design of fast and efficient next generation wireless communication techniques [7]. An inertial

Manuscript received March 20, 2020; revised July 14, 2020 and December 7, 2020; accepted March 25, 2021. Date of publication April 5, 2021; date of current version December 9, 2021. This work has received funding from Infotech Oulu, the EU Horizon 2020 (No 761794, TERRANOVA) and from the Academy of Finland 6Genesis Flagship (grant 318927). The associate editor coordinating the review of this article and approving it for publication was M. Erol-kantarci. (*Corresponding author: Zaheer Khan.*)

Zaheer Khan and Janne J. Lehtomäki are with the Faculty of Information Technology and Electrical Engineering, University of Oulu, 90120 Oulu, Finland (e-mail: zaheer.khan@oulu.fi).

Valerio Selis is with the Department of Electrical and Electronics Engineering, University of Liverpool, Liverpool L69 3GJ, U.K.

Hamed Ahmadi is with the Department of Electronic Engineering, University of York, York YO10 5DD, U.K.

Alan Marshall is with the Department of Electrical Engineering and Electronics, University of Liverpool, Liverpool L69 3GJ, U.K.

Digital Object Identifier 10.1109/TCCN.2021.3071142

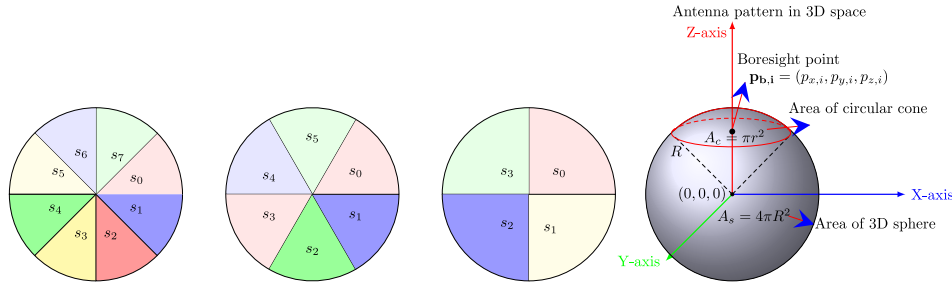


Fig. 1. Examples showing heterogeneous circular sectors (heterogeneous beamwidths) in 2D space and also an example showing a spherical sector within a 3D sphere. The 3D sphere represents the total combined coverage of all spherical sectors.

measurement unit (IMU) generally contains three orthogonal rate-gyroscope sensors and three orthogonal accelerometer sensors. By processing signals from these gyroscopes and accelerometers, it is possible to track the position and orientation of a device or an object in a 3D space. An important contribution of this work is to investigate how these sensors could be used to assist fast and efficient user link maintenance/rediscovery in wireless networks using directional antennas. Our main contributions in this work can be summarized as following:

- We present discovery methods for users using reconfigurable directional antennas under: 1) an infrastructure network scenario, where  $N - 1$  users are user devices and the  $N$ th user is an access point; and 2) an ad hoc network scenario, where all  $N$  users are user devices.
- We provide both analytical and simulation results for the proposed methods. We evaluate the proposed methods in terms of time-to-discovery (TTD), which is the amount of time (typically measured in time steps) that it takes for two users to discover each other using their directional antennas, once they have begun the discovery process. We show that one of the two proposed methods is optimal in terms of TTD.
- We then focus on the problem of rediscovering the communication link which is degraded/lost due to rotational motion of a user and/or its device. We formulate it as an antenna beam prediction problem in a 3D space. We propose sensor assisted rediscovery methods which exploit simple techniques proposed by us to predict beam directions in which a device should search to rediscover the link between two users.
- To evaluate the performance of the proposed methods in terms of time-to-rediscovery (TTR), we considered changes in the orientation of antenna radiation beams in 3D space. We have used real datasets describing changes in a user device's orientation patterns which in turn are used to model changes in orientation of directional antenna beams. Our results show that using the proposed beam prediction methods a user can successfully rediscover the lost link with close to 100% accuracy by searching only in two different directions. This reduces the number of time steps required to rediscover links by  $S_x$  ( $S$  times), where  $S$  is the number of antenna sectors, as compared to otherwise repetitive

discovery search over a large number of different beam directions.

## II. RELATED WORK

It is worth noting that in the past there have been several studies relating to the potential use of directional antennas in ad hoc networks [8], [9]. However, the importance of using directional antennas to overcome high attenuation in mmWave communications has gained attention more recently [4], [10], [11]. The authors in [12] highlight the challenges incurred in mmWave frequencies for an infrastructure-based network where users need to establish/discover a link with a base station. When directional antennas are studied for use in ad hoc networks, some works refer to the process of user discovery as neighbor discovery [13]. It is important to note that most works which have studied the problem of user/neighbor discovery using directional antennas have modeled antenna radiation pattern in a particular direction as a two dimensional (2D) circular sector (see [13], [14], and the references therein). From a handheld device/computer perspective, it is more appropriate to model an antenna beam feature as a three-dimensional (3D) sector [15] (for an example, see Fig. 1). Moreover, the works in [13] and [14] have made the unrealistic assumption in which each user can utilize a distinct sequence within the same type of sequence group. This is unrealistic as users remain unaware about the sequences used by the other users until they achieve discovery with each other. Our methods do not assume that each user can have a distinct sequence and our methods perform well under orientation changes in a device. Moreover, some other works have the strong assumption that users have the assistance of the global positioning system (GPS) which is utilized to achieve highly accurate synchronization which in turn is used to achieve fast discovery by pointing in a certain direction at the same time [16], and [17]. When the assumptions of GPS and compass are removed then the proposed method in [17] is almost reduced to random selection (RS) of antenna sectors for discovery.

Our methods do not assume such GPS assistance as GPS may not be always available, e.g., it does not work indoors, and also it consumes a lot of device battery if often required to be turned ON. It is worth noting that there are several works which assume that users can also configure their antenna to omnidirectional or quasi-omnidirectional

mode [18], [19], [20]; however, our work focuses only on users using directional antennas at both ends. Our approach is more practical because at mmWave and teraHertz frequencies both ends need to be directional to overcome the large path losses. If one end would use omnidirectional mode, this would lead to a mismatch between communication range and discovery range. Our work also does not assume that users are static, hence, we not only propose user discovery methods but also provide solutions to the problem of subsequent link rediscovery/maintenance with IMU sensor assisted predictions. To evaluate the performance of the proposed link rediscovery methods we use real datasets describing changes in a user device's orientation patterns. The works in [21] and [10] have used compressive sensing based techniques to study user discovery process. However, the compressive sensing has not been used to study user discovery process for the networks where both transmit and receive ends are using directional mode and where only one directional sector can be used for transmit/receive at a time instant. Our work is different from the compressive sensing based discovery techniques as it considers directional antenna for both transmit/receive ends.

The work in [22] has studied 3D statistical channel model for mmWave, and [15] has studied connectivity trade-offs in 3D wireless sensor networks using directional antennas. The work in [23] considers directional antenna orientation model in 3D space and an algorithm is proposed which can calculate the pointing angles for a non-horizontal aligned antenna. However, the algorithm proposed in [23] focuses only on satellite communications. The use of smart sensor/data assisted techniques to efficiently solve various radio resource management problems have also attracted the use of such techniques for wireless networks in other contexts. For example, some recent works [24], [25] have used motion sensors on mobile devices to estimate device attitude or they have used them to estimate smartphone rotation. In this work, we use motion sensors to facilitate directional link maintenance/rediscovery.

### III. SYSTEM MODEL

Typically, a wireless network can be an ad hoc or an infrastructure-based. In an infrastructure-based network multiple users communicate via a common entity called access point (AP), whereas in an ad hoc network multiple users can communicate directly with each other. Under both network scenarios, we consider a generic reconfigurable antenna, where reconfigurability means that an antenna can generate a beam which can be switched in different directions. Our work focuses on a challenging scenario where a user can only transmit/receive in one direction at a time. The generic directional antennas considered in this work can generate beams in  $S$  different directions, where  $\mathcal{S} = \{s_0, s_1, \dots, s_{(S-1)}\}$  is the set of all antenna sectors (see Fig. 1 for illustrative examples). This generic directional antenna model is widely considered in fundamental research analysis relating to directional antennas (see [13], [26], and the references therein). We also use  $s_{i,j}$  to represent the  $i$ th sector of the  $j$ th user in the network, and  $\psi_{jk}$  is used to denote the sector that user  $j$  is using to successfully communicate with another user  $k$ . Without loss of generality,

for the derivation of closed-form solutions and tractability we consider that  $|\mathcal{S}_j| = |\mathcal{S}|$ , i.e., to be same among all  $N$  users and is denoted by  $S$ . However, our proposed discovery/rediscovery methods are equivalently valid for the heterogeneous cases, where heterogeneity is in terms of number of antenna sectors among the users.

In 2D, under a generic directional antenna model, the communication range of a user can be divided into  $S = M$  circular sectors. To cover the entire 2D circular space we need a reconfigurable antenna that can generate a directional beam which spans an angle  $\alpha_M = 2\pi/M$  radians and which can be switched in  $M$  different directions. For a directional beam in 3D space, we may approximate the main lobe or main antenna beam in a particular direction as a spherical cone which intersects the sphere of radius  $R$ . The radius  $R$  can be considered as the maximum distance from a source at which effective communication can take place. In Fig. 1, we illustrate examples showing antennas with heterogeneous sectors. In the figure, an example of 8, 6 and 4 circular sectors and also an example of a spherical sector are presented. In 3D, under a generic directional antenna model, the communication range of a user can be divided into  $D$  cones, i.e.,  $S = D$  spherical sectors, in which each cone ‘‘cuts out’’ an area  $A_s$  of a sphere and it represents a different direction in which the directional antenna can be switched to generate a beam (see Fig. 1). We can then define the beam solid angle  $\Omega_D$  of a directional antenna as the solid angle through which most of the power of the antenna would flow.

*Observation 1:* It is important to note that  $D > M$ , i.e., the number of spherical sectors required to cover the entire 3D space of a sphere with radius  $R$  is greater than the number of sectors that can cover a circle with the same radius  $R$ . For example, in a typical 2D circular sector model,  $M = 2\pi/\alpha_M$  directional beams are required to cover the entire circular space of radius  $R$ . When each of these  $M$  beams is modeled to cover an area equal to that of a spherical cone area then the total area covered by the  $M$  such spherical cones is given by

$$A_T = \frac{2\pi}{\alpha_M} A_i \quad (1)$$

where

$$A_i = \pi R^2 \sin^2\left(\frac{\alpha_M}{2}\right), \quad (2)$$

However, the total area of a sphere with radius  $R$  is  $A_s = 4\pi R^2$ . The ratio between  $A_s$  and  $A_T$  can be calculated as

$$R_A = \frac{4\alpha_M}{2\pi \sin^2\left(\frac{\alpha_M}{2}\right)} \quad (3)$$

It can be seen that  $R_A > 0$  for  $\alpha_M > 0$ .

Observation 1 is important as it means that a user discovery method which searches over  $M$  sectors based on a popular 2D space modeling will not cover all directions in a practical 3D space model leading to holes in user search in some directions. This in turn can result in a reduced probability of successful discovery for handheld devices/computers. To cover the whole 3D space of a sphere, in our work we have used the Tammes problem formulation [27]. There can be still some small gaps for the case of a conical directional beam which spans an angle

$\Omega_D = 4\pi/D$  steradian. However, when some beam overlapping is allowed then a directional beam which spans an angle slightly greater than  $\Omega_D$  can be used to cover the entire 3D spherical space. For the case where even the overlapping parts have enough signal strength for user discovery, then it is better for the proposed methods as now the discovery can happen in more than one sector. This will only reduce the TTD/TTR of the proposed directional link discovery/rediscovery algorithms.

#### IV. USER DISCOVERY/REDISCOVERY USING DIRECTIONAL ANTENNAS

We define user discovery as the process by which two or more users discover one another with signal power level above the minimum detection threshold,  $T_d$ . In general, there are beacon (discovery) periods at some fixed interval which are dedicated for the purpose of user discovery. These periodic discovery periods ensure that a user who wants to establish a communication link with another user can make it happen. Each period lasts a few milliseconds and is followed by a data transmission period. It is reported in [20] that the exact duration of beacon plus data transmission periods can be chosen by the system designer and it can be chosen to be in the range of 100 ms to 1000 ms. In our work, the time step duration represents a single time unit within each beacon period which is typically defined in a wireless standard, such as IEEE 802.11ad, to make sure that there is enough time to receive/transmit discovery frame and acknowledgement of it. The time step duration is considered to be 100  $\mu$ s and the work in [28] studying mmWave techniques also considers the same time step duration. Further more, it is reported in [28] (and references therein) that round trip latency in mmWave products ranges from 20  $\mu$ s to around 200  $\mu$ s which means that our use of 100  $\mu$ s is an appropriate choice. Hence, the duration of a beacon period is simply 100  $\mu$   $\times$  the number of time steps.

We do not assume that the two users know that they should discover each other. Let's say during the discovery phase a user  $i$  in a given time step using the selected antenna sector listens on the medium for the presence of another user (in ad hoc mode). If it does not sense others in its vicinity or it does not receive a beacon signal, the user will transmit a beacon signal, and will listen for a response. On receiving the response from a user  $i'$ , user  $i$  can start to establish a communication link if the user  $i'$  is a desired user. For the infrastructure mode, the user listens in a given time step for an AP beacon signal and responds to it on receiving the signal. The AP can then start to establish a communication link if the user is a desired user. A user may need to scan the  $S$  sectors multiple times which can lead to a large number of discovery steps. This makes the problem of autonomously finding a suitable antenna direction for users a challenging one. Illustrative examples of periodic discovery periods and a time step duration are presented in Fig. 3.

In a typical wireless network, a MAC frame type is represented by using a few bits (which identify the type of the frame, such as beacon and etc) in predefined part of the frame control field of the MAC header. For example, bits 1000 can

be used to ID a beacon frame and 1101 can be used to ID an ACK frame. In this way a beacon packet can be distinguished from the other packets. We evaluate the discovery methods for users with directional antennas in terms of TTD. The average TTD in second(s) is given by

$$\bar{t}_d = E[TTD] \times t_s \quad (4)$$

where  $E[TTD]$  is the expected number of time steps required, and  $t_s$  is the duration of a single time step. Unit of each time step  $t_s$  is seconds and is considered to be 100  $\mu$ s, without loss of generality. Our considered time step duration is based on what other works in this area have reported, for example the work studying mmWave communications in [28] (and also the references therein). Using  $E[TTD]$  and  $t_s$  one can obtain expected time duration till discovery in seconds for a proposed method.

Let  $E_s$  denote the event where two users attempt to discover each other. Note that it is possible that two users start the discovery period at the same time, we call such a discovery process as the synchronous discovery process. However, there can be a lag  $\tau$  between the time that user  $i$  and user  $j$  start the discovery period, we call such a discovery process as the asynchronous discovery process. Users can get synchronized once they successfully communicate beacon packets via the use of Time Synchronization Function (TSF) which is also described in relevance to mmWave networks following the IEEE 802.11ay standard [29]. Once two users have discovered each other using particular antenna sectors, then changes in orientation of a user/device can become a critical issue. This is due to the reason that such changes can introduce translational and/or rotational effects which may cause either the utilized sectors for directional communication to be misaligned or they may point in completely different directions. This can result either in high packet loss (link degradation) or complete loss of communication.

Typically, in a wireless network both sides use some time out value after which when the link quality remains degraded or remains lost the communicating users will need to initiate the rediscovery process. The work in [30] suggest the time out value to be Timeout = Estimate of RTT + 4  $\times$  Deviation. The round trip time (RTT) in our work is considered to be 100  $\mu$ s [28]. Further more, it is reported in [28] (and references therein) that round trip latency in mmWave products ranges from 20  $\mu$ s to around 200  $\mu$ s and states that use of 100  $\mu$ s is an appropriate choice. Hence, assuming uniform distribution the time out value to initiate the rediscovery process in our work is considered to be  $T_o = 100 + 4 \times \sqrt{1/12(200 - 20)^2} \approx 400 \mu$ s.

In Fig. 2a, we illustrate an example in 2D space where a user 1 discovers another node using sector  $s_{5,1}$ . In Fig. 2b due to rotation of node's device along the xy plane now sector  $s_{0,1}$  points in the direction in which previously  $s_{5,1}$  was pointing. However, without rediscovery or orientation tracking the node will still utilize sector  $s_{5,1}$  for communication which can result in either high packet loss or complete loss of communications. In Figs. 2c and 2d, we illustrate and explain the possible impact of change in device orientation under the 3D spherical sector model. A simple solution to this is to perform user discovery again after every time

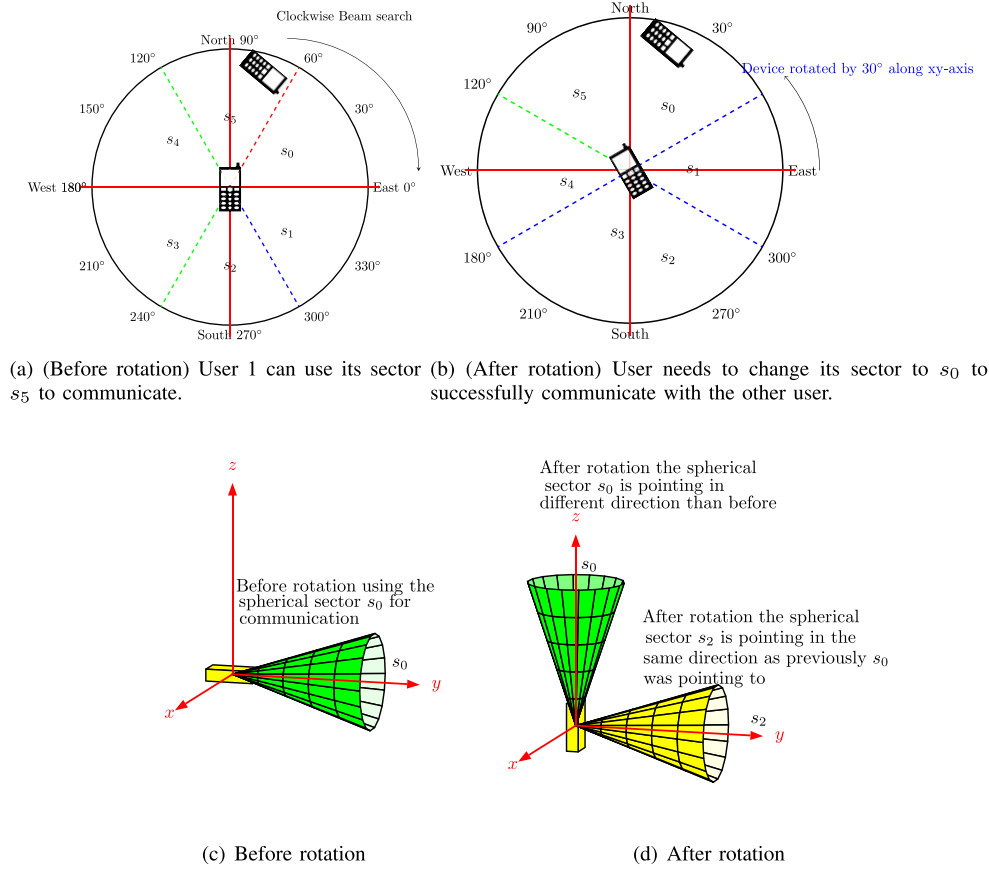


Fig. 2. Examples illustrating the impact of change in device orientation under the 2D and the 3D models.

link degrades or loss of communications occurs. However, as degradation or loss in communication due to changes in device orientation can often occur, repeating user discovery method which involves scanning through all large number of antenna sectors can incur significant user discovery overhead (and communication latency). Wireless users equipped with directional antennas may exploit sensor-assisted intelligent orientation tracking methods to perform link rediscovery that reduces the overhead and latency incurred due to repetitive search over a large number of antenna sectors. We also evaluate the performance of the proposed rediscovery methods in terms of TTR. This is the number of time steps taken to rediscover directional links after initial discovery when translational and/or rotational effects may cause their communication to degrade or to be lost. The average TTR in second(s) is given by

$$\bar{t}_m = E[TTR] \times t_s \quad (5)$$

where  $E[TTR]$  is the expected number of time steps required to rediscover.

## V. USER DISCOVERY ALGORITHMS

Next, we present methods using which users can accomplish discovery.

1) *Random Scan (RS) Algorithm:* In a random antenna scan, a user scans its antenna sectors in random order. During each time step, the user  $j$  will select any of the  $s_{i,j}$  antenna

### Algorithm 1 RS Algorithm

---

**Initialize:** User  $j$  is activated // a user wants to establish a link to communicate with another user  
**while** not discover OR not rediscover link **do**  
     $i = \text{randi}[0, S-1]$   
    attempt to discover using the antenna state  $i$ , i.e.,  $s_{i,j}$   
**end while**

---

sector with probability  $1/S$ . For two users following this method, discovery will be achieved when two select those antenna sectors  $s_{i,j}$  and  $s_{i',j'}$  that allow them to correctly direct the beam towards each other in a way that they can successfully communicate. In the next time steps, the two users communicate using the same  $s_{i,j}$  and  $s_{i',j'}$ . Algorithm 1 describes the steps in more detail.

Let  $E_d$  denote the event that, in a given time step, both users select their antenna sector which allows each to successfully communicate with the other. It is easy to see that under the RS method the probability that the event  $E_d$  will happen is given by

$$P\{E_d\} = \frac{1}{S^2} \quad (6)$$

Using the well-known result for Bernoulli processes the  $E[TTD]$  is given by

$$E[TTD] = \frac{1}{P\{E_d\}} = S^2. \quad (7)$$



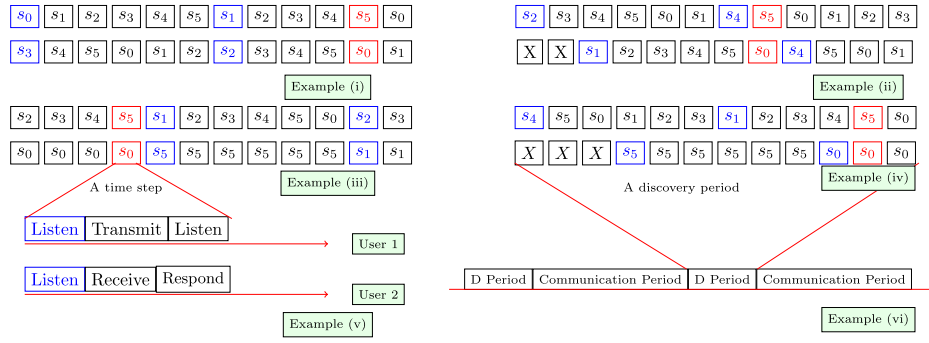


Fig. 3. i) and iii) illustrate the synchronous discovery case. User 1 and user 2 have completed discovery when user 1 scans  $s_5$  and user 2 scans  $s_0$  at the same time (red color time steps). ii) and iv) illustrate discovery under the asynchronous case where two users start the discovery process with some time lag  $X$ . v) illustrates successfully completed discovery process within a given time step, and vi) illustrates periodic discovery periods.

TABLE I  
E[TTD] AS A FUNCTION OF NUMBER OF SECTORS FOR THE RS METHOD

Number of sectors	$S = 3$	$S = 6$	$S = 9$	$S = 12$
$E[TTD]$	9	36	81	144

#### A. An Optimal Method for Infrastructure-Based Network

We show that when an AP and user nodes use two different strategies (as given in Algorithm 2), this enables them to discover each other in an expected number of time steps of  $\frac{(S^2+1)}{2}$  which is almost half as compared to the RS.

To explain the Algorithm 2 in simple words: an AP uses a sequence of length  $L$  which can be constructed by an initial random selection of a row from the matrix  $S_m$  and then repeating it  $\frac{L}{S}$  times. The user node constructs the  $L$  length sequence by an initial random selection of a row from the matrix  $S_m$ , performing a Kronecker product on it with a vector of length  $S$  whose all-elements are 1, and then repeating it  $\frac{L}{S^2}$  times. The matrix  $S_m$  is an  $S \times S$  matrix whose rows are composed of cyclically shifted versions of  $S$  of antenna sectors. For example, the  $4 \times 4$  circulant matrix on the set  $S = \{s_0, s_1, s_2, s_3\}$  is given by

$$S_m = \begin{matrix} & \begin{matrix} \rho_3 & \rho_2 & \rho_1 & \rho_0 \end{matrix} \\ \begin{matrix} \rho_3 \\ \rho_2 \\ \rho_1 \\ \rho_0 \end{matrix} & \begin{pmatrix} s_3 & s_0 & s_1 & s_2 \\ s_2 & s_3 & s_0 & s_1 \\ s_1 & s_2 & s_3 & s_0 \\ s_0 & s_1 & s_2 & s_3 \end{pmatrix} \end{matrix} \quad (8)$$

Fast and slow state in Algorithm 2 means how often you switch the antenna sector to scan. In the fast scan state, the antenna sector scan is switched more often as compared to the slow scan state.

**Proposition 1:** When an AP and a user node use different strategies then the expected value of time steps required to discover is at least  $\frac{(S^2+1)}{2}$  and the maximum number of time steps to discovery is no more than  $S^2$ . This is achieved by a method called fast slow circulant sequence (FSCS) and is given in Algorithm 2.

**Proof:** The proof is inspired by the search strategy for multiple locations Lemma in [31]. Suppose that a user knows that using the antenna state  $\hat{s}_i$  it will discover an AP  $i$  but the AP  $i$  does not know using which state it will discover the user. The two nodes can have guaranteed discovery within  $S$  time

#### Algorithm 2 Fast Slow Circulant Sequence Based Scan Algorithm

**Initialize:** User  $j$  is activated // a user wants to establish a communication link with the AP  
 $\rho = (s_0, \dots, s_{S-1})$  // antenna state indices  
 $S_m = \text{circmat}\{\rho\}$  // circulant matrix generation of antenna state indices  
**if** AP: STATE=FAST **then**  
 $k = \text{randi}[0, S-1]$  // random selection of circulant matrix row index  
 $\Psi_j = \text{repeat}(\rho_k, S)$  // generate the sequence by repeating  $\rho_k$  row of the matrix  $S$  times  
 $i = 1$  // initialize index  $i$  of the sequence  $\Psi_j$   
**while** not discover OR not rediscover link **do**  
    attempt to discover in a time step using antenna state given in  $\psi_{i,j}$ , i.e., the  $i$ th element of  $\Psi_j$   
     $i = i + 1 \bmod L$  //  $L$  is the length of the sequence and mod is modulus  
**end while**  
**else if** User Device: STATE=SLOW **then**  
 $k = \text{randi}[0, S-1]$  // random selection of circulant matrix row index  
 $\Psi_j^a = \rho_k \otimes \text{ones}(S)$  // generate the sequence by taking kronecker product of row  $\rho_k$  with a vector of length  $S$  whose all-elements are 1  
**while** not discover OR not rediscover link **do**  
    attempt to discover in a time step using antenna state given in  $\psi_{i,j}$ , i.e., the  $i$ th element of  $\Psi_j^a$   
     $i = i + 1 \bmod L$   
**end while**  
**end if**

steps, and the number of time steps to discovery are  $\frac{(S+1)}{2}$  in expected value. This is achieved by the strategy in which the user listens using the state  $\hat{s}_i$  in every time step while the AP  $i$  randomly selects a row of the matrix  $S_m$  and attempts discovery in the order given in the selected sequence.

$$P\left(\bigcup_{j=1}^t E_j\right) \leq \min\left\{1, \sum_{j=1}^k P(E_j)\right\} = \min\left\{1, \frac{k}{S}\right\} \quad (9)$$

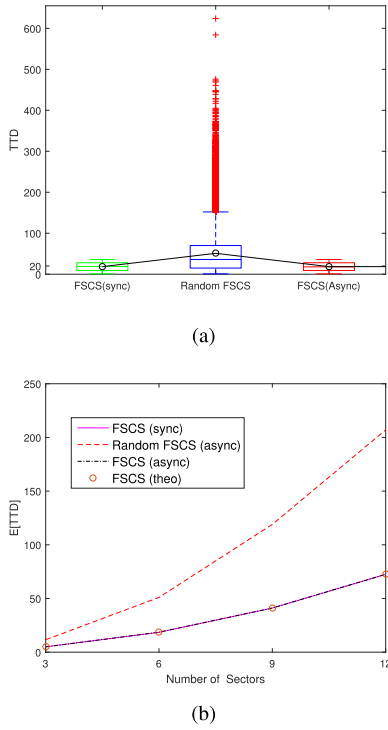


Fig. 4. a) Boxplots showing TTD in time steps for various methods under different scenarios; b)  $E[TTD]$  in time steps as a function of sectors. FSCS then denote the results obtained via closed-form equation in Eq. (11).

When we relax the assumption that the user knows the antenna state  $\hat{s}_i$  then it is easy to see that the probability two nodes discover each other (event  $E$ ) within  $\hat{t}$  time steps is

$$P\left(\bigcup_{j=1}^{\hat{t}} E_j\right) \leq \min\left\{1, \sum_{j=1}^{\hat{t}} P(E_j)\right\} = \min\left\{1, \frac{\hat{t}}{S^2}\right\} \quad (10)$$

The bound on the right-hand side is achieved by the method given in Algorithm 2. It is easy to see that the  $E[TTD]$  is given by

$$E[TTD] = \left(\frac{(1 + 2 + \dots + S^2)}{S^2}\right) = \frac{(S^2 + 1)}{2}. \quad (11)$$

**Remark 1:** It should be clear that it is important for a user  $i$  and also the AP to generate their sequences as described in Algorithm 2 as not any sequence can achieve the same performance. Particularly for the case where users are not synchronized and one can start the discovery process before or after the other. For example, consider the case where unlike Algorithm 2 the  $\Psi_i$  is constructed by an AP  $i$  by performing  $\frac{L}{S}$  times a random selection of a row from  $\mathbf{S}_m$ . For the case, where AP  $i$  starts the discovery process  $\tau = 1$  time step after the other there is strictly greater than zero probability that the discovery process will take more than  $S^2$  time steps for the AP  $i$ . However, for Algorithm 2 it is still no more than  $S^2$  time steps for the user  $i$ .

In Fig. 4a, we quantize this observation by plotting the boxplots of the TTD results for both FSCS (sync) and FSCS (async). It can be seen that the proposed method is not affected

by asynchronicity in users' discovery. The box plots of the TTD in Fig. 4a are plotted for each method under different network scenarios and each user using  $S = 6$  sectors. Moreover, the boxplot results are obtained from simulations by performing  $R = 40000$  Monte Carlo (MC) runs. In each run, presented TTD results are obtained where each user utilizes a sequence of 1000 steps which is constructed using one of the presented methods. The lag value  $\tau$  to model asynchronous discovery is generated randomly with uniform probability. Note that when users are homogeneous (each user employs an antenna with the same number of sectors), then this random selection is from  $[0, 1, \dots, S - 1]$ , where  $S$  is the number of sectors. When the users are not homogenous, then this random selection is from  $[0, 1, \dots, LCM(S_1, S_2, \dots)]$ , where  $LCM()$  represents the least common multiple of the number of antenna sectors of users.

In each figure, the bottom and the top edges of the box indicate the 25th and 75th percentiles. The whiskers in each figure extend to the most extreme data points not considered outliers, the outliers (if any) are plotted in each figure individually using the '+' symbol, and mean is plotted using the 'o' symbol. It can also be seen from Fig. 4a that the median is centered in the boxes for both the sync and the async FSCS cases, it shows no skewness in the sample and the mean and the median coincide. The median TTD is 18.5 time steps and the maximum TTD is 36 time steps. Note that the maximum TTD of FSCS method is equal to the mean TTD value of  $S^2 = 36$  for the RS method (Algorithm 1). To show that not any sequence will work, we also compare the performance with a case where the AP and the user instead of repeating search scans as proposed in the FSCS method, perform some random search scans with repetitions as explained in Remark 1. We call this method as random FSCS. In Fig. 4b, we plot the  $E[TTD]$  for a user and its AP as a function of the number of directional antenna sectors. We evaluate the performance of the proposed FSCS method under both synchronous and asynchronous scenarios and also compare its performance with the random FSCS method. It can be seen from the figure that in terms of  $E[TTD]$  for  $S = 12$  antenna sectors the proposed method outperforms the random FSCS method by almost 200 time steps. Moreover, one can see from Table I and Fig. 4b that for  $S = 12$  the proposed FSCS method outperforms the RS method by almost 90 time steps. Our results show that even though when there can be a lag  $\tau$ , the two users can eventually discover each other. Since using the proposed FSCS method, an AP and a user is guaranteed to discover each other within bounded time which means that its boxplot has all the values within the whiskers (most extreme points) and it has no outliers. Contrary to this, for the random FSCS method although most of the values are within the whiskers, however, it can take even as high as 600 or more time steps leading to having outliers.

In Fig. 4b, we also compare the results given by the closed-form expression we derived in Eq. (11) for the proposed FSCS method (denoted by FSCS theo in the figure) and the  $E[TTD]$  from a Monte Carlo simulation. Observe that the  $E[TTD]$  from Monte-Carlo simulations are within  $\pm 1\%$  of those obtained from Eq. (11).

**Algorithm 3** Shifted Circulant Sequence-Based Algorithm

---

**Initialize:** User  $j$  is activated // a user wants to establish a communication link with another user  
 $\rho = s_0, \dots, s_{M-1}$  // antenna state indices  
 $\mathbf{S}_m = \text{circmat}\{\rho\}$  // circulant matrix generation of antenna state indices  
 $\Psi_j = \text{seq}(\text{randi}(\text{row}(\mathbf{S}_m)), l)$  // select randomly  $l$  times a row from  $\mathbf{S}_m$  to construct the sequence  
 $\hat{\tau} = \text{randi}[0, S-1]$  // select a random value  $\hat{\tau}$  for the sequence shift  
 $\Psi_j^s = \text{circshift}(\Psi_j, \hat{\tau})$  // shift the sequence  
**while** not discover OR not rediscover link **do**  
    attempt to discover in a time step using antenna state given in  $\psi_{i,j}$ , i.e., the  $i$ th element of  $\Psi_j^s$   
**end while**

---

### B. Shifted Circulant Sequence-Based Discovery in an Ad Hoc Network

Unlike the infrastructure case, in the ad hoc case pre-assignment of roles, where one user selects to be always in the fast scan state and the other user selects to be in the slow scan state can be difficult to achieve. Where the pre-assignment of roles is not possible then each user can utilize the Shifted Circulant Sequence-based (SCS) method. The steps involved in the method are presented in Algorithm 3. The idea is that users search using the arbitrarily delayed version of the same sequence. We shall see next that it is a good idea to shift (by value  $\hat{\tau}$ ) a sequence that is obtained via random selection of rows from a circulant matrix.

**Proposition 2:** When two users attempt discovery using the Algorithm 3 but each use a sequence called  $\Psi_j^c$  which is constructed from a random selection of circulant matrix rows (but with no shift by value  $\hat{\tau}$ ) then from  $t = 1$  expected time to discovery is  $E[TTD] = [S(S-1) + (\sum_{n_s=1}^S \frac{n_s}{S})]$ .

**Proof:** Lets' say any two users will successfully discover each other when in a given time step a user  $j$  selects sector  $s_{i,j}$  and the user  $j'$  selects sector  $s_{i',j'}$ . In a random selection of a row from the matrix  $\mathbf{S}_m$ , the probability that the two users select a particular row pair in which  $(s_{i,j}, s_{i',j'})$  can be scanned at the same time at its first element is  $\frac{1}{S^2}$ . Similarly, the probability that the two users select a particular row pair in which  $(s_{i,j}, s_{i',j'})$  can be scanned at the same time at its second element is also  $\frac{1}{S^2}$ , and so on. For  $S$  number of sectors, there are  $S$  such row pairs in which  $(s_{i,j}, s_{i',j'})$  can be scanned at the same time at  $S$  distinct elements. Hence, in each independent random selection of a row, the probability that any two users select any row pair in which  $(s_{i,j}, s_{i',j'})$  are scanned in the same time step (but at distinct elements) is  $\frac{1}{S^2} \times S$ .

Let  $\hat{E}$  denote the event that the two users select a row pair which allow them to scan  $(s_{i,j}, s_{i',j'})$  in the same time step. Under a single attempt of random row selection by each user, the probability that the event  $\hat{E}$  will happen is given by  $P\{\hat{E}\} = \frac{1}{S}$ . From  $P\{\hat{E}\}$  and the fact that  $(s_{i,j}, s_{i',j'})$  occur at  $S$  distinct elements, the  $E[TTD]$  is given by

$$E[TTD] = \left[ S(S-1) + \left( \sum_{n_s=1}^S \frac{n_s}{S} \right) \right], \quad (12)$$

As the sequence  $\Psi_j^c$  is constructed by performing  $\frac{L}{S}$  times independent random selection of a row from matrix  $\mathbf{S}_m$  the expected TTD given above is achieved by it for sufficiently large  $L$ . ■

In claiming that using  $\Psi_j^s$  in Algorithm 3 gives better performance than  $\Psi_j^c$  we have observed that its expected TTD is less than given in Eq. (12). The reason is as follows. For a sequence  $\Psi^c$  of length  $L$ , the probability of achieving successful discovery at its  $L$ th step can be calculated as

$$P\{E_{d,L}\} = \frac{1}{S} \left[ \sum_{j=1}^{\frac{L}{S}} \left( 1 + \frac{1}{S} \right)^j \right] \quad (13)$$

We know that the sum term in Eq. (13) is a finite geometric series with ratio  $r = 1 - \frac{1}{S}$ , so it can be rewritten as

$$P\{E_{d,L}\} = \frac{1}{S} \left[ \frac{1 - \left( 1 - \frac{1}{S} \right)^{\frac{L}{S}+1}}{1 - \left( 1 - \frac{1}{S} \right)} \right] = \left[ 1 - \left( 1 - \frac{1}{S} \right)^{\frac{L}{S}+1} \right] \quad (14)$$

For a sequence  $\Psi^s$  of length  $L$ , the probability of achieving successful discovery at its  $L$ th step is

$$P\{E_{d,L}\} = \left[ 1 - \left( 1 - \frac{1}{S} \right)^{\frac{L}{S}+1} \right] + \epsilon \quad (15)$$

where  $\epsilon > 0$  as shift (by the  $\hat{\tau}$  value) increases the number of ways in which the two users can discover each other. Quantifying  $\epsilon$  for any  $L$  is difficult to obtain but for  $L = 2S$  we have  $\epsilon = \frac{(2S-1)}{S^4}$ . This is because for  $L = 2S$  out of total  $S^4$  possibilities there are  $(2S-1)$  more ways for the users to discover each other as compared to when the sequence is not shifted.

It can be seen in Fig. 5a that the mean value for the SCS (async) is 32.8 steps, and for the SCS (sync) it is 33.1 steps. The SCS method also performs better than the RS method. In Fig. 5b, we present boxplots showing TTD results for the proposed SCS and FSCS methods when a directional antenna with  $S = 24$  sectors is utilized. In Fig. 5c, we plot the  $E[TTD]$  as a function of the number of antenna sectors. We evaluate the performance of the proposed SCS method under both synchronous and asynchronous scenarios and also compare its performance with the randomized version of the SCS method. It can be seen that the proposed method slightly outperforms the methods which involve randomized SCS selection. In the same figure, we also compare the results given by the closed-form expression we derived in Eq. (12) (which serves as an upper bound for the proposed SCS method) and the  $E[TTD]$  from an MC simulation. Observe that the  $E[TTD]$  from MC simulations are within  $\pm 1\%$  of those obtained from Eq. (12).

Successful discovery is not only guaranteed by selecting an appropriate sequence length  $L$  for the discovery in a given discovery period but also by having periodic discovery periods at some fixed intervals. As in each discovery period, these methods enable discovery with high probability this means that over multiple periods the probability of not being able to discover approaches 0. For these methods which provide discovery with high probability, the sequence length  $L$  in a



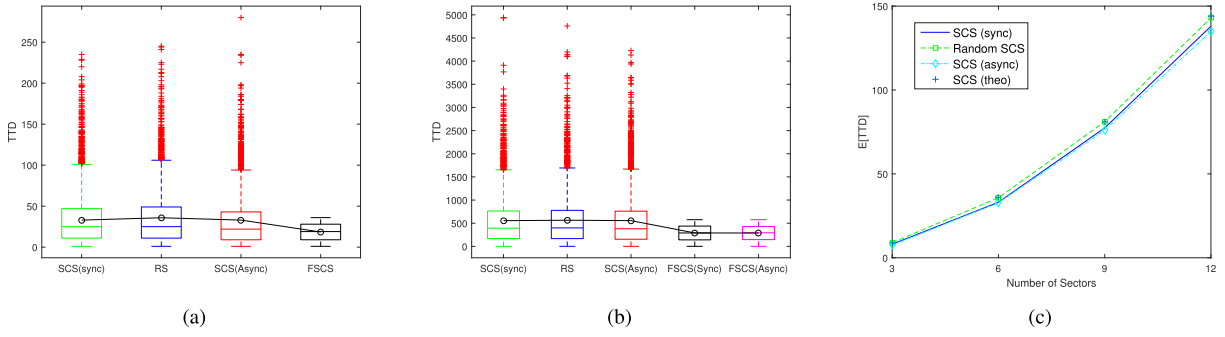


Fig. 5. a) Boxplots showing TTD in time steps ( $S = 6$  sectors) for the proposed methods and also the RS method; b) Boxplots showing TTD in time steps ( $S = 24$  sectors).

discovery period should be equal to at least their  $E[TTD] + 2\sigma$  where  $\sigma$  represents the standard deviation value.

### C. Comparison With Other Methods

It is important to note that not every method can outperform RS based directional discovery. In fact the work in [13] has studied how the directional discovery algorithm can be configured to achieve a desired trade-off between average and worst-case discovery delay performance. It is shown that to minimize the worst-case delay the average delay performance of the proposed algorithm in [13] will be degraded. It is also shown in [13] that on average the algorithm performs worse than the RS based discovery.

An oblivious neighbor discovery algorithm for directional antenna users is proposed in [13]. The algorithm assumes that each user can utilize a distinct sequence within the same type of sequence group. This is a strong assumption as users remain unaware about the sequences used by the other users until they achieve discovery with each other. The proposed method in [13] achieves guaranteed discovery within a bounded delay. The work in [13] also demonstrates how the directional discovery algorithm can be configured to achieve a desired trade-off between average and worst-case discovery delay performance. It is shown that to minimize the worst-case delay the algorithm's average delay performance will be degraded and on average the algorithm performs worse than the random antenna sector selection (RS) based discovery. However, it is important to note that unlike the method in [13], the RS method does not provide guaranteed discovery. In Fig. 6a, we compare the performance of the oblivious discovery algorithm of [13] with our proposed FSCS and SCS discovery algorithms under the same scenarios as considered in [13]. It can be seen from the figure that our proposed method's worst case delay and also the average delay are significantly less than the method proposed in [13]. Moreover, our proposed FSCS method provides guaranteed user discovery in no more than  $S^2$  steps. This means that the worst case delay of our proposed scheme is equal to the average delay of the RS method in [17]. Moreover, it can be seen that in terms of average delay the proposed SCS method performs better than both RS and Oblivious discovery methods.

Using GPS assistance, a fully synchronized search based directional antenna discovery approach has been proposed

in [17]. However, unlike our work, the work in [17] only provides performance evaluation in terms of average discovery delay and the proposed method in [17] cannot provide any guaranteed discovery bound. In Fig. 6b, we compare the performance of the GPS assisted discovery algorithm of [17] with our proposed FSCS and SCS discovery algorithms under the same scenarios as considered in [17]. It can be seen from the figure that our proposed FSCS algorithm performs better than the GPS-assisted technique proposed in [17]. It can be also seen that the method of [17] performs better than the RS method. It is important to note that if GPS availability is always assumed like the work in [17], then our proposed SCS method will also perform slightly better than the method of [17]. This is due to the reason that in [17] it is assumed that using GPS users can be synchronized so that they point to the same direction (let's say North) with exactly the same antenna sector. This synchronization for the proposed SCS method will mean that each user instead of performing random selection of a sequence can use the same sequence for each search. This will improve the performance in terms of discovery delay. In Fig. 6c we present comparison results with the Enhanced Handshake discovery method of [26]. It can be seen from Fig. 6c that the EHandshake method gives higher average  $[TTD]$  than our proposed FSCS method. Moreover, Fig. 6c shows that while for  $S = 6$  sectors the difference in average  $[TTD]$  performance between our proposed FSCS and EHandshake is 15 time steps, when the number of sectors is increased to 24 then this difference significantly increases to 276 time steps. Moreover, it can also be seen from the figure that EHandshake performs always slightly better than the RS method.

In the next section, we present sensor-assisted rediscovery methods and their performance evaluation results and show that for the proposed FSCS method the maximum TTR in time steps is no more than  $2S$  and average TTR is  $\frac{2S+1}{2}$ . This is a significant reduction in delay as for the TTD the maximum value was  $S^2$  and the average was  $\frac{S^2+1}{2}$ . Moreover, for the proposed SCS method the average TTR is  $\frac{(S+1)}{2} + S$ . This is again reduction in delay as for the TTD the average value was slightly less than  $S^2$ . It is important to note that all the methods in [13], [17], [26] require full search for rediscovery making  $TTR = TTD$ .

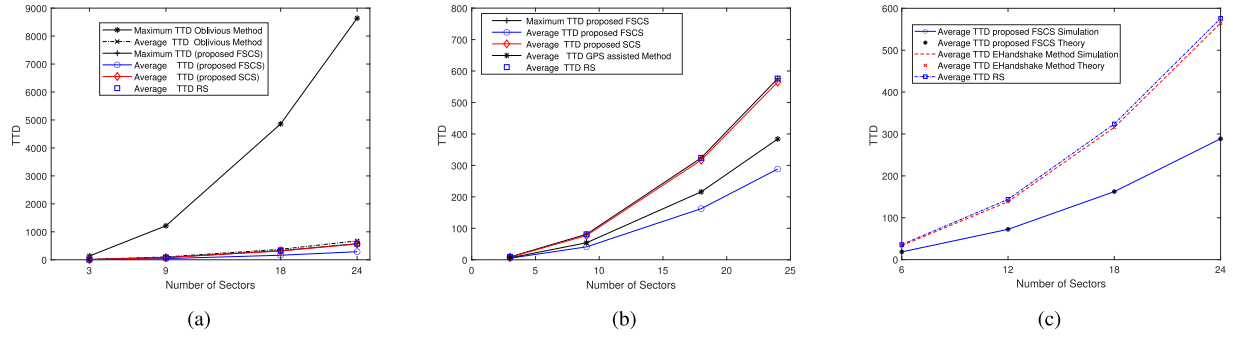


Fig. 6. Comparison of TTD in time steps as a function of number of antenna sectors for various methods.

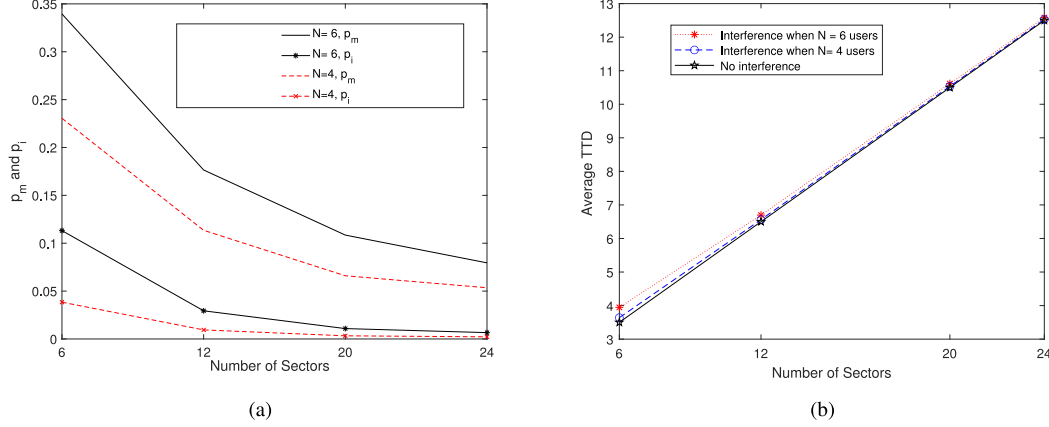


Fig. 7. a) Probability  $p_i$  as a function of number of antenna sectors; b) In the presence of interference, average TTD in time steps as a function of number of sectors for the SCS method.

#### D. Interference Impact on User Discovery

In a wireless network, when two or more users perform discovery, the probability of having some interference among these users is inevitable. In the proposed algorithms, the probability of interference is minimized by incorporating three features: i) in each discovery period, our proposed algorithms generate antenna sector scan sequences in a way which ensures that for each user there is randomization in the antenna scanning order given in the selected sequence. This randomization minimizes the probability of interference  $p_i$ , as it decreases the probability that a user is receiving using the sector  $s_i$  and one or more potentially interfering users transmit at the same time towards the sector  $s_i$ ; ii) in each time step of a discovery period a user  $i$  using the selected antenna sector listens on the medium for the presence of another user (in ad hoc mode). If it does not sense others in its vicinity or it does not receive a beacon signal, the user will transmit a beacon signal, and will listen for a response. Whereas in an infrastructure mode, an AP transmits the beacons and the user devices listen to them, the user devices only listen in a given time step of each discovery period for an AP beacon signal and responds to it on receiving the signal; and iii) A discovery period is periodically repeated at fixed interval. When due to interference two users are unable to discover each other during the first discovery period, there is possibility for them to discover in the subsequent discovery periods.

The probability of having some interference in a network can only increase TTD and eventually users will discover each other. We confirm our this observation by including results showing TTD in the presence of interference probability  $p_i$ . Using extensive simulations, we calculated the probability that a receiving user's sector is in the transmitting range of one or more potentially interfering users' sectors. We denote this probability by  $p_m$ . To obtain the probability of interference  $p_i$ , we need to multiply the  $p_m$  with the probability  $p_t$  which is the probability that the user is receiving using the sector  $s_i$  and one or more potentially interfering users transmit at the same time towards the sector  $s_i$ . In Fig. 7a, we present the probability of interference  $p_i$  as a function of the number of sectors. Results in Fig. 7a are obtained using simulations running over 10000 Monte Carlo runs in which 6 users (3 users transmitting to 3 receiving users) are randomly dropped in a network site of radius 30 meters. The figure also shows the results relating to the deployment of 4 users (2 users transmitting to 2 receiving users). The results in the figure confirm that as the number of sectors is increased the  $p_i$  is decreased. For  $S = 6$  sectors it can be seen from the figure that  $p_i$  is 0.11 for 6 users case and its 0.04 for 4 users case. It can also be seen that for  $S = 24$  sectors the  $p_i$  is significantly reduced to 0.02 for 6 users case and 0.01 for 4 users case. It can be seen from Fig. 7a that as the number of antenna sectors is increased then the probability of interference  $p_i$  is decreased and for  $S = 24$  sectors the  $p_i$

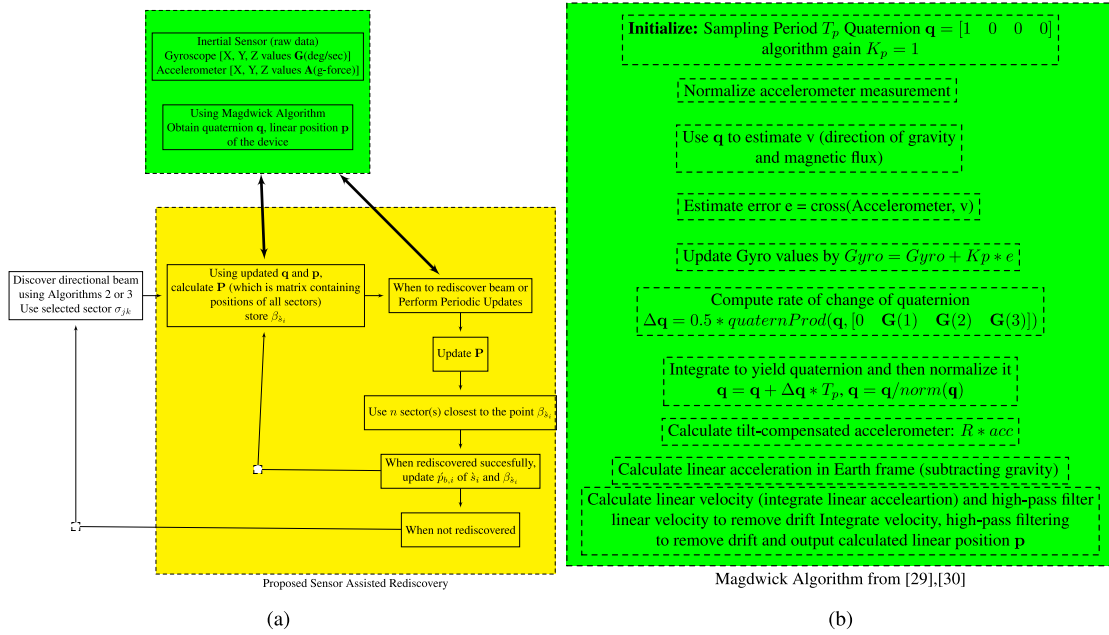


Fig. 8. Predictions based sensor assisted rediscovery method.

is less than 2%. It can be also seen from Fig. 7b that there is some impact of interference on average TTD for  $S = 6$  sectors and the impact is negligible for the higher number of sectors. The results in Fig. 7b are based on extensive simulations in which 6 users (3 users transmitting to 3 receiving users) and 4 users (2 users transmitting to 2 receiving users) are randomly dropped in a network site of radius 30 meters.

## VI. PREDICTIONS BASED SENSOR ASSISTED REDISCOVERY

As directional antennas focus energy in a particular direction, one frequent cause of link loss can be due to orientation changes. For example, orientation can change due to the way how a user places it on a surface, or due to the way the user holds the device in a certain way. Moreover, if there is a change in the orientation of the user itself this can also change the device orientation. In Figs. 2 and 9, we provide illustrative examples of how rotations in a 2D and a 3D space can lead to a loss in the communication link between two users under both infrastructure and ad hoc cases. Embedding an efficient IMU sensor in a user's device and fusing/processing their raw data using an efficient algorithm can help estimate rotation and translation of mobile devices. When rediscovery is required to perform then instead of scanning through a large number of antenna sectors, the estimated rotation and position can be used to predict which antenna sectors to be used for scanning/searching for rediscovering the users. Our focus in this work is on how an IMU can be used to predict which antenna sectors to be used for link rediscovery and how many sectors are required to be searched to achieve close to 100% accuracy.

To represent the rotation of a device in 3D space we need some parametrization. Various mathematical constructs, such as rotation matrices and quaternions, are used to represent the orientation/rotation of a rigid body in 3D space.

Quaternions are most commonly utilized as they are simple to use, they are excellent for interpolation, and do not suffer from Gimbal lock which is the loss of one degree of freedom in a 3D space [32], [33]. Next we present some details of how a quaternion is used for rotation estimation.

### A. Quaternion Background

A quaternion may be represented as

$$\mathbf{q} = q_0 + \mathbf{q}_v = q_0 + \mathbf{i}q_1 + \mathbf{j}q_2 + \mathbf{k}q_3 \quad (16)$$

where  $\mathbf{i}, \mathbf{j}, \mathbf{k}$  are the standard orthonormal basis in a 3D coordinatized plane, denoted  $R^3$ . In the above sum,  $q_0$  is called the scalar part of the quaternion while  $\mathbf{q}_v$  is called the vector part of the quaternion. We can define the complex conjugate of the quaternion  $\mathbf{q}$  to be the quaternion, denoted  $\mathbf{q}^*$ , given by

$$\mathbf{q}^* = q_0 - \mathbf{q}_v = q_0 - \mathbf{i}q_1 - \mathbf{j}q_2 - \mathbf{k}q_3 \quad (17)$$

A quaternion whose scalar part is zero is defined as a pure quaternion, i.e., it is of the form  $(0, \mathbf{q}_v) = 0 + \mathbf{i}q_1 + \mathbf{j}q_2 + \mathbf{k}q_3$ . The norm of a quaternion  $\mathbf{q}$ , denoted by  $|\mathbf{q}|$  is the scalar  $|\mathbf{q}| = \sqrt{\mathbf{q}^* \mathbf{q}}$ . A quaternion is called unit quaternion if its norm is 1. In 2D, the multiplication of two complex numbers implies 2D rotation. However, for the 3D case, the quaternion operator  $L_q(\mathbf{v})$  may be interpreted as a vector rotation, given by

$$\begin{aligned} L_q(\mathbf{v}) &= \mathbf{q}\mathbf{v}\mathbf{q}^* = (q_0 - \mathbf{q}_v)\mathbf{v}(q_0 + \mathbf{q}_v) \\ &= (2q_0^2 - 1)\mathbf{v} + 2(\mathbf{v} \cdot \mathbf{q})\mathbf{q} + 2q_0(\mathbf{v} \times \mathbf{q}) \end{aligned} \quad (18)$$

where  $\mathbf{v} \in R^3$  can simply be treated as though it were a pure quaternion  $\mathbf{q} \in R^4$ . Expanding each of the terms in Eq. (18):  $(2q_0^2 - 1)\mathbf{v}$ ,  $2(\mathbf{v} \cdot \mathbf{q})\mathbf{q}$ , and  $2q_0(\mathbf{v} \times \mathbf{q})$  we get three matrices. Then the sum of these three matrices from Eq. (18) can be

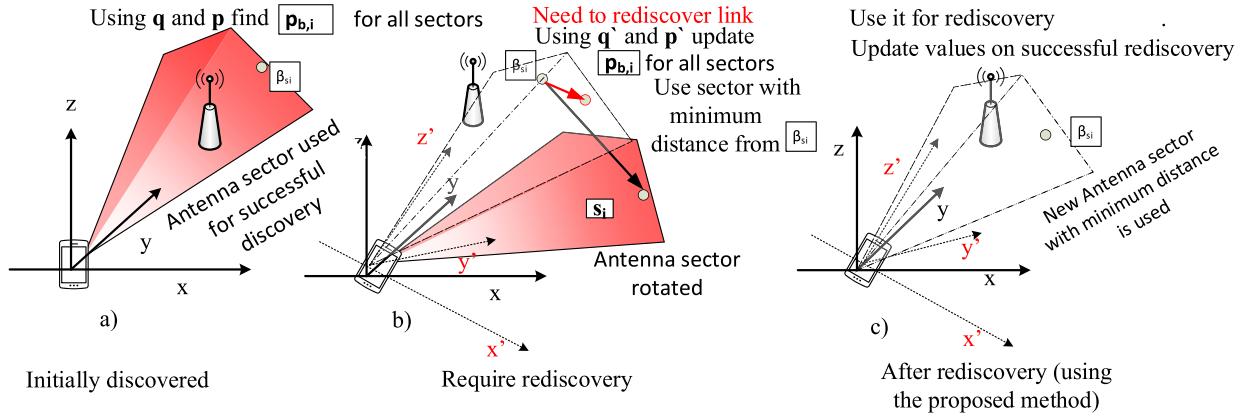


Fig. 9. An example illustrating how the proposed rediscovery works.

given as

$$\mathbf{w} = L_q(\mathbf{v}) = \begin{bmatrix} 2q_0^2 - 1 + 2q_1^2 & 2q_1q_2 + 2q_0q_3 & 2q_1q_3 - 2q_0q_2 \\ 2q_1q_2 - 2q_0q_3 & 2q_0^2 - 1 + 2q_2^2 & 2q_2q_3 + 2q_0q_1 \\ 2q_1q_3 + 2q_0q_2 & 2q_2q_3 - 2q_0q_1 & 2q_0^2 - 1 + 2q_3^2 \end{bmatrix} \begin{bmatrix} v_1 \\ v_2 \\ v_3 \end{bmatrix}. \quad (19)$$

The above equation simply means that when quaternion rotation operator is applied to vector  $\mathbf{v}$  (a pure quaternion defined in the reference frame) then it can be expressed as  $\mathbf{w}$  in the rotated frame.

#### B. Steps Involved in the Prediction of Antenna Sectors for Rediscovery

In Fig. 8, we present important steps involved in the proposed sensor assisted predictions based rediscovery method. To help better understand the proposed method, we also provide an illustrative example showing the process of discovery and rediscovery in Fig. 9.

Let us denote the center point of each spherical cone  $i$  at distance  $R$  from its radiation source as  $\mathbf{p}_{b,i} = (p_{x,i}, p_{y,i}, p_{z,i})$ . We call this point as *boresight point* as it is lying on antenna boresight line which is the axis of maximum gain (maximum radiated power) of a directional antenna (see Fig. 1). We next explain the important steps involved in the proposed method in details:

- Initialize the position of the boresight point  $\mathbf{p}_{b,i}$  of each directional antenna sector  $s_i$  of a device. In order to describe the initial boresight point positions, one can consider each point to be lying on the surface of a 3D sphere whose center is at position  $\mathbf{p} = (0, 0, 0)$ , and a  $z$ -axis (up) device coordinate system is attached to it. The 3D sphere represents the total combined coverage of all spherical sectors. One can then use the sensor data from IMU and the Magdwick algorithm (see Fig. 8) to proceed to describe the position and orientation of this device coordinate system with respect to the world coordinate system [34], [35].
- Denote the antenna sector which is used to discover user  $k$  as  $s_i$ . Using the IMU sensor data and the Magdwick algorithm (see Fig. 8), update the boresight point position

$\mathbf{p}_{b,i}$  of  $s_i$  and also of all other boresight points using

$$\dot{\mathbf{p}}_{b,i} = \dot{\mathbf{p}} + \mathbf{M}\mathbf{p}_{b,i} \quad \forall i \in \mathcal{S} \quad (20)$$

where  $\dot{\mathbf{p}}_{b,i}$  is the updated boresight point position,  $\dot{\mathbf{p}}$  is the updated center position of the sphere, and  $\mathcal{S}$  is the set of all antenna sectors. Store the updated boresight point position of sector  $s_i$  as  $\beta_{s_i}$ .

- **Minimum Distance-Based Predictions:** When required to rediscover the directional link then update the current positions of all boresight points using Eq. (20). Find the distance between  $\beta_{s_i}$  (position of the sector's boresight point which was last time successfully used for communication) and the updated positions of each of the boresight points. Sort the distances in ascending order and select  $n$  sectors with minimum distance values, where  $n$  is a parameter (number of predicted sectors which should be searched) and  $n \in [1, S]$ . In the subsequent paragraph, we present results where we vary the value for  $n$  between 1 and 2 (out of total 12 sectors) to evaluate the performance of the proposed method in terms of probability of successful rediscovery. Note that the decision to rediscover beam can be based on some performance criteria, such as when the received signal falls below a predefined threshold value, or when the packet loss exceeds some predefined packet loss threshold value.
- When rediscovered successfully using one of the  $n$  sectors then update  $s_i$  and  $\beta_{s_i}$  to the new values of the sector which is now used for successful discovery/communications.
- When not rediscovered use the proposed FSCS or the SCS algorithms to perform scan through all  $S$  sectors.
- **Smoothing-Based Predictions:** In this approach, when there is degradation in the predefined performance criteria, the prediction of  $n$  antenna sectors to be used in scan search is calculated by multiplying past values by relative weights, which are calculated based upon what can be termed a smoothing parameter  $\alpha$ . When a sector is utilized for successful discovery/rediscovery, we denote that time as  $t = 0$  and its position is by  $X_0$ , the specific formula for this smoothing then is given as

$$X^0 = \beta_{s_i}^0, \text{ for } t = 0$$





Fig. 10. IMU sensor utilized for the collection of real datasets for various rotation patterns of a hand held device.

$$X^t = \alpha X^{t-1} + (1 - \alpha)\beta_{s_i}^t, \text{ for } t = 0 \quad (21)$$

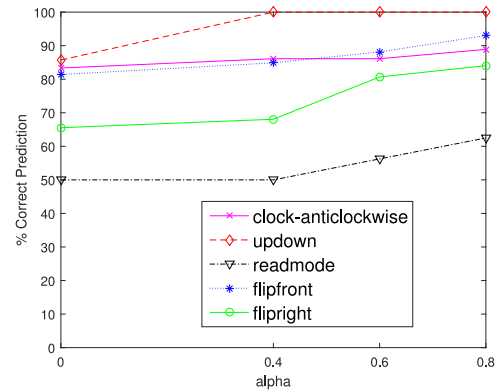
This can be viewed as the magnitude of the weight applied to the previous values, with the weights decreasing exponentially as the observations get older. It is easy to see that when  $\alpha = 0$ , this method is equal to the minimum distance-based method. Hence, the only extra overhead in the smoothing-based method as compared to the minimum distance-based method is that it needs only to remember the previous value  $X^{t-1}$  plus there is one extra multiplication and addition operation.

- When the received signal falls below a predefined threshold value, or when the packet loss exceeds the predefined packet loss threshold value then to rediscover the user instead of finding the minimum distance between each of the updated boresight point positions and the  $\beta_{s_i}^t$ , now we find the minimum distance between  $X^t$  and the updated boresight point positions. The distances are sorted in ascending order and  $n$  selected sectors with minimum distance values are used for rediscovery, where  $n$  is again a parameter and  $n \in [1, S]$ . We will present results in the subsequent paragraph which show that the past values used in this approach can reduce the number of antenna sectors used for rediscovery.
- When rediscovered successfully update  $\beta_{s_i}$  to the new value of the sector, set  $t = 0$  and restart the smoothing process given in Eq. (21).
- When not rediscovered use the proposed FSCS or SCS algorithms to perform scan through all  $S$  sectors.

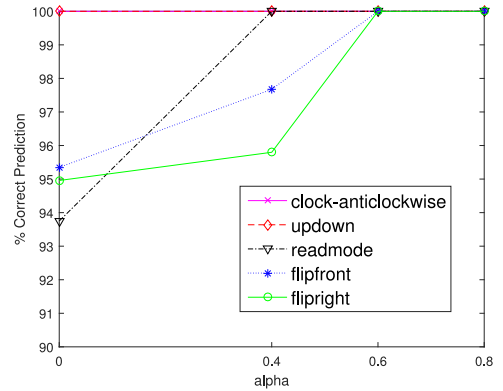
The proposed IMU sensor-based discovery method is for both infrastructure-based networks and ad hoc networks. However, the performance evaluation results presented in the next subsection are for the scenarios where user at one end changes orientation while the other user remains fixed, such as in an infrastructure-based network where an AP is fixed while a user can change orientation or in an ad hoc network where only one user has changed its orientation. For the ad hoc networks case where users at both ends may change their orientation then both the users may need to perform orientation tracking. This is a more challenging scenario and is the topic of our future research.

### C. Performance Evaluation Using Real datasets

We evaluate the effectiveness of our proposed methods by testing them with real datasets representing various device rotation patterns in a 3D space. The real datasets used in the results were collected using ADIS16365 IMU device attached to a handheld device. The IMU device along with



(a)  $n = 1$



(b)  $n = 2$

Fig. 11. Correct predictions in percentage using the proposed sensor assisted method.

its data collection module utilized are shown in Fig. 10. We collected multiple datasets representing various typical rotational/movements that a handheld device can encounter. For example, in Dataset1 (called clock-anticlockwise), we rotated several times the device with the attached IMU in clockwise and anticlockwise directions, in Dataset2 (called Updown), we moved the handheld device several times in up and down directions, in Dataset3 (called readmode), we held the device in read mode and then moved it from left to right, in Dataset4 (called flipfront) we flipped the device several times front to back and vice versa, and in Dataset4 (called flipright) we flipped the device several times from left to right and vice versa.

The performance metric we use is the number of times in percentage the proposed methods correctly predict which antenna sector to be used after the directional link is lost between two users due to changes in orientation. If the predicted antenna sector can enable successful communication, we count it as a success else we count a failure. We call the performance metric as the percentage of correct predictions ( $P_C$ ). We consider the directional link to be lost when the antenna sector beam which is used to discover/communicate turns 30% or more of the beam solid angle  $\Omega_D$ . In Fig. 11a, we present the performance evaluation results for  $n = 1$  when there are  $S = 12$  directional sector beams covering the entire 3D spherical space. Setting the parameter  $n = 1$  means that

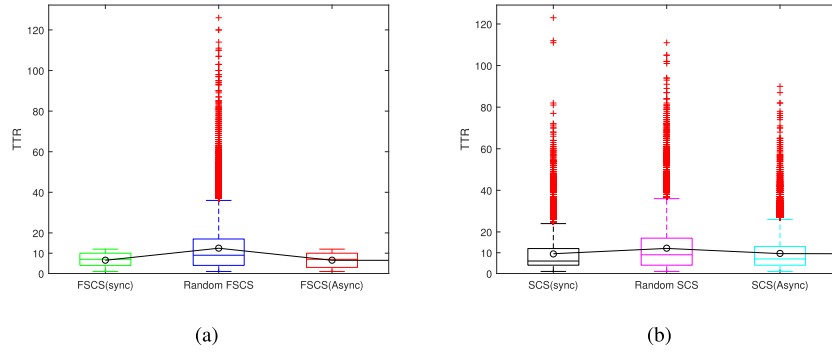


Fig. 12. Boxplots showing TTR in time steps for various methods using sensor assisted prediction based rediscovery.

the proposed methods are allowed to predict only one antenna sector out of  $S = 12$ , which is to be used for rediscovery. In Fig. 11b, we present the performance evaluation results for  $n = 2$  also which means that now the proposed methods can predict two antenna sectors which are to be used for rediscovery. Fig. 11a shows that for  $n = 1$  the prediction accuracy of the minimum distance-based rediscovery ( $\alpha = 0$ ) is between 82% to 87% for the collected datasets 1, 2 and 4. It also can be seen from the same figure that the smoothing based rediscovery can increase the prediction accuracy and for  $\alpha = 0.8$  the prediction accuracy is between 90% to 100% for the same datasets. When  $\alpha = 0$ , the prediction accuracy is 67% for the dataset 5, whereas  $\alpha = 0.8$  can increase the prediction accuracy to 83%. For the dataset 3,  $\alpha = 0$  gives the prediction accuracy of 50% and  $\alpha = 0.8$  can increase the prediction accuracy to 62%. Fig. 11a also shows that the highest prediction accuracy is reached for  $\alpha = 0.8$ . Fig. 11b shows that for  $n = 2$  the prediction accuracy of the minimum distance-based rediscovery ( $\alpha = 0$ ) increases to 100% for the collected datasets 1, and 2, and for datasets 3, 4, and 5 the prediction accuracy increases to at least 93%. It can also be seen from the same figure that the smoothing based rediscovery can increase the prediction accuracy to 100% for all the 5 datasets. Both Fig. 11a and Fig. 11b also shows that the highest prediction accuracy is reached for  $\alpha = 0.8$ .

We next evaluate the performance in terms of TTR of the proposed methods with sensor assisted rediscovery. We consider the case where the two users need to rediscover the link as one of the two users have rotated and the discovered link is lost. The rotated user utilizes  $n = 2$  antenna sectors predicted for rediscovery whereas the other user (who has not rotated) utilizes all  $S$  antenna sectors for rediscovery. In Figs. 12a–b, boxplots of the TTR are plotted for each method presented in Section V under different network scenarios and  $S = 6$  antenna sectors. Moreover, the boxplot results are obtained from simulations by performing  $R = 30000$  MC runs. In each run, one user rotates randomly, uses  $n = 2$  predicted antenna sectors for rediscovery. Figs. 12a and 12b show that when the proposed antenna sector prediction is used then the  $E[TTR]$  is less than 10 steps for both the FSCS and the SCS methods. It can also be seen that the maximum TTR of the proposed FSCS method is no more than 12 steps, and for the SCS method the maximum TTR value is within 90 steps for the rediscovery.

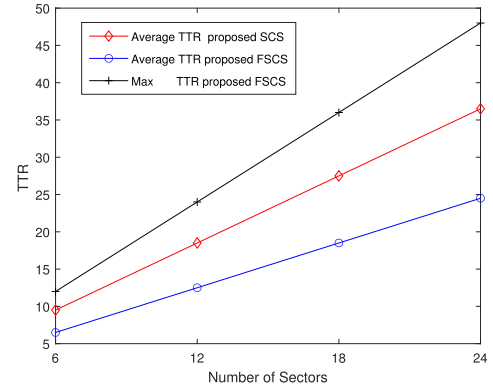


Fig. 13. TTR in time steps as a function of number of sectors.

These numbers are once again at least twice less than the maximum TTR values given in Figs. 4 and 5.

We provide some closed form expressions which can be used to obtain numerical values for the TTR related results, such as the results given in Fig. 12. For the proposed FSCS method, when rediscovery is performed using search in  $n = 1$  predicted sector then  $E[TTR] = \frac{S+1}{2}$  and maximum TTR in steps is no more than  $S$ . For the same method, when rediscovery is performed using search in  $n = 2$  predicted sectors then  $E[TTR] = \frac{2S+1}{2}$  and maximum TTR is no more than  $2S$ . The benefit of using search in  $n = 2$  predicted sectors is that for the utilized real datasets representing more than six different rotation patterns it gave 100 percent prediction accuracy for the sensor assisted rediscovery method presented in Section VI. For the SCS method, when rediscovery is performed using  $n = 1$  predicted sector then  $E[TTR] = \frac{S+1}{2}$ . When rediscovery is performed using  $n = 2$  predicted sector then  $E[TTR] = \frac{(S+1)}{2} + S$ . In Fig. 13, for  $n = 2$  predicted sectors, we verify the closed form expressions by using simulations and plot the TTR in steps as a function of number of directional antenna sectors. It can be seen from the figure that for the proposed FSCS method the maximum TTR in time steps is no more than  $2S$  and average TTR is  $\frac{2S+1}{2}$ . This is a significant reduction in delay as for the TTD the maximum value was  $S^2$  and the average was  $\frac{S^2+1}{2}$ . Moreover, in the same figure, for the proposed SCS method the average TTR is  $\frac{(S+1)}{2} + S$ . The simulated results in the figure confirm the validity of the presented closed-form expressions.



## VII. CONCLUSION AND FUTURE DIRECTIONS

The aim of this paper was to design efficient methods to achieve communication link discovery for wireless hand-held devices utilizing directional antennas. As the discovered link can be lost due to a user/device rotation and/or mobility, our paper also proposed methods that enable users to rediscover quickly without the need of scanning in a large number of different antenna directions. Both infrastructure and ad hoc wireless networks using directional antennas are considered in our work. Two link discovery methods were presented and their performance in terms of time to discovery (TTD) was evaluated using both analytical and simulation results. We also compared their performance with various other discovery methods. The proposed fast slow circulant sequence (FSCS) method provides guaranteed link discovery in an infrastructure-based network with no more than  $S^2$  time steps and takes on average  $\frac{S^2+1}{2}$  time steps to discover a link, where  $S$  is the number of directional antenna sectors. Several other works have assumed that each user can utilize a distinct sequence based on a unique short ID or they have assumed that the user always has the assistance of the global positioning system (GPS) available to accurate synchronization. We do not make such assumptions, however, when such extra feature is assumed then our proposed FSCS method also provides guaranteed link discovery in an ad hoc network. For ad hoc networks, we have proposed the shifted circulant sequence (SCS) method. This method allows faster expected TTD in an ad hoc network as compared to the randomized scanning method. Similarly, when extra features, such as availability of a distinct sequence or GPS support, is assumed then our proposed SCS method significantly improves performance in terms of TTD.

Focusing energy in a particular direction creates challenges as a user and/or its device orientation can frequently change which can lead to the discovered link being lost. To address the challenge, we proposed an inertial measurement unit (IMU) assisted fast and efficient rediscovery methods. Based on IMU data, the proposed methods predict the specific directions in a 3D space in which a user should search to rediscover the link. Using real collected datasets representing various changes in a device, we evaluated the prediction performance of the proposed methods. We showed that using our proposed sensor assisted prediction technique as few as two predicted antenna beams (sectors) are enough to search for a user to successfully rediscover a directional link with probability 1. Moreover, the delay due to rediscovery time is reduced by  $S$  times as compared to the discovery time, where  $S$  is the number of antenna sectors.

There are multiple ways in which this research can be extended. For example, one possible extension is to take into account the impact of motion on the proposed IMU assisted rediscovery methods and to enhance them to perform efficiently under motion as well. Another possible extension is to consider the impact on discovery algorithms of various types of overlapping directional antenna beams using more realistic directional antenna models.

## REFERENCES

- [1] "5G spectrum recommendations," Bellevue, WA, USA, 5G Americas, White Paper, Apr. 2017. [Online]. Available: [http://www.5gamericas.org/files/9114/9324/1786/5GA\\_5G\\_Spectrum\\_Recommendations\\_2017\\_FINAL.pdf](http://www.5gamericas.org/files/9114/9324/1786/5GA_5G_Spectrum_Recommendations_2017_FINAL.pdf)
- [2] "mmWave: The battle of the bands," Austin, TX, USA, National Instruments, White Paper, Jun. 2016. [Online]. Available: <http://www.ni.com/white-paper/53096/en/>
- [3] K. Tekbiyik, A. R. Ekti, G. K. Kurt, and A. Gorcin, "Terahertz band communication systems: Challenges, novelties and standardization efforts," *Phys. Commun.*, vol. 35, p. 12, Aug. 2019. [Online]. Available: <http://www.sciencedirect.com/science/article/pii/S1874490718307766>
- [4] X. Yu, J. Zhang, M. Haenggi, and K. B. Letaief, "Coverage analysis for millimeter wave networks: The impact of directional antenna arrays," *IEEE J. Sel. Areas Commun.*, vol. 35, no. 7, pp. 1498–1512, Jul. 2017.
- [5] Y. S. Eroglu, C. K. Anjinappa, I. Guvenc, and N. Pala, "Slow beam steering and NOMA for indoor multi-user visible light communications," *IEEE Trans. Mobile Comput.*, vol. 20, no. 4, pp. 1627–1641, Apr. 2021.
- [6] Y. Kaymak, R. Rojas-Cessa, J. Feng, N. Ansari, M. Zhou, and T. Zhang, "A survey on acquisition, tracking, and pointing mechanisms for mobile free-space optical communications," *IEEE Commun. Surveys Tuts.*, vol. 20, no. 2, pp. 1104–1123, 2nd Quart., 2018.
- [7] A. W. Doff, K. Chandra, and R. V. Prasad, "Sensor assisted movement identification and prediction for beamformed 60 GHz links," in *Proc. 12th Annu. IEEE Consum. Commun. Netw. Conf. (CCNC)*, 2015, pp. 648–653.
- [8] H.-N. Dai, K.-W. Ng, M. Li, and M.-Y. Wu, "An overview of using directional antennas in wireless networks," *Int. J. Commun. Syst.*, vol. 26, no. 4, pp. 413–448, 2013.
- [9] H. Koubaa, "Reflections on smart antennas for MAC protocols in multihop ad hoc networks," in *Proc. European Wireless*, Florence, Italy, Feb. 2002, p. 7.
- [10] M. E. Rasekh, Z. Marzi, Y. Zhu, U. Madhoo, and H. Zheng, "Noncoherent mmwave path tracking," in *Proc. 18th Int. Workshop Mobile Comput. Syst. Appl.*, 2017, pp. 13–18.
- [11] G. Bielsa, A. Loch, I. Tejado, T. Nitsche, and J. Widmer, "60 GHz networking: Mobility, beamforming, and frame level operation from theory to practice," *IEEE Trans. Mobile Comput.*, vol. 28, no. 10, pp. 2217–2230, Oct. 2019.
- [12] M. Giordani, M. Mezzavilla, C. N. Barati, S. Rangan, and M. Zorzi, "Comparative analysis of initial access techniques in 5G mmWave cellular networks," in *Proc. Annu. Conf. Inf. Sci. Syst. (CISS)*, Mar. 2016, pp. 268–273.
- [13] L. Chen, Y. Li, and A. V. Vasilakos, "On oblivious neighbor discovery in distributed wireless networks with directional antennas: Theoretical foundation and algorithm design," *IEEE/ACM Trans. Netw.*, vol. 25, no. 4, pp. 1982–1993, Aug. 2017.
- [14] Z. Zhang and B. Li, "Neighbor discovery in mobile ad hoc self-configuring networks with directional antennas: Algorithms and comparisons," *IEEE Trans. Wireless Commun.*, vol. 7, no. 5, pp. 1540–1549, May 2008.
- [15] E. Kranakis, D. Krizanc, A. Modi, and O. Morales-Ponce, "Connectivity trade-offs in 3D wireless sensor networks using directional antenna," in *Proc. IEEE Int. Parallel Distrib. Process. Symp.*, May 2011, pp. 345–351.
- [16] W. Zhang, L. Peng, R. Xu, L. Zhang, and J. Zhu, "Neighbor discovery in three-dimensional mobile ad hoc networks with directional antennas," in *Proc. 25th Wireless Opt. Commun. Conf. (WOCC)*, 2016, pp. 1–5.
- [17] J.-S. Park, S.-W. Cho, M. Y. Sanadidi, and M. Gerla, "An analytical framework for neighbor discovery strategies in ad hoc networks with sectorized antennas," *IEEE Commun. Lett.*, vol. 13, no. 11, pp. 832–834, Nov. 2009.
- [18] C. N. Barati *et al.*, "Directional cell discovery in millimeter wave cellular networks," *IEEE Trans. Wireless Commun.*, vol. 14, no. 12, pp. 6664–6678, Dec. 2015.
- [19] M. Khan, S. Bhunia, M. Yuksel, and S. Sengupta, "LOS discovery in 3D for highly directional transceivers," in *Proc. IEEE Military Commun. Conf. (MILCOM)*, 2016, pp. 325–330.
- [20] B. Satchidanandan, S. Yau, P. R. Kumar, A. Aziz, A. Ekbal, and N. Kundargi, "TrackMAC: An IEEE 802.11ad-compatible beam tracking-based MAC protocol for 5G millimeter-wave local area networks," in *Proc. 10th Int. Conf. Commun. Syst. Netw. (COMSNETS)*, 2018, pp. 182–185.

- [21] D. Steinmetzer, D. Wegemer, M. Schulz, J. Widmer, and M. Hollick, "Compressive millimeter-wave sector selection in off-the-shelf IEEE 802.11ad devices," in *Proc. 13th Int. Conf. Emerg. Netw. Exp. Technol.*, New York, NY, USA, 2017, pp. 414–425. [Online]. Available: <https://doi.org/10.1145/3143361.3143384>
- [22] M. K. Samimi and T. S. Rappaport, "3D statistical channel model for millimeter wave outdoor mobile broadband communications," in *Proc. IEEE Int. Conf. Commun. (ICC)*, Jun. 2015, pp. 2430–2436.
- [23] TUM and Eutelsat, "Calculation of azimuth, elevation and polarization for non-horizontal aligned antennas," document TD-1205-a, The Entrepreneurial University–TUM, Munich, Germany, 2016. [Online]. Available: <https://www.eutelsat.com/files/contributed/support/pdf/azimut-h-elevation-polarization.pdf>
- [24] S. Ayub, A. Bahraminasab, and B. Honary, "A sensor fusion method for smart phone orientation estimation," in *Proc. 13th Annu. Post Grad. Symp. Converg. Telecommun. Netw. Broadcast.*, Jun. 2012, pp. 1–5.
- [25] P. Zhou, M. Li, and G. Shen, "Use it free: Instantly knowing your phone attitude," in *Proc. 20th Annu. Int. Conf. Mobile Comput. Netw. (MobiCom)*, 2014, pp. 605–616.
- [26] X. An, R. V. Prasad, and I. Niemegeers, "Neighbor discovery in 60 GHz wireless personal area networks," in *Proc. IEEE Int. Symp. 'World Wireless Mobile Multimedia Netw.' (WoWMoM)*, 2010, pp. 1–8.
- [27] D. Weaire and T. Aste, *The Pursuit of Perfect Packing*. Boca Raton, FL, USA: CRC Press, 2000. [Online]. Available: <https://books.google.fi/books?id=5scgCAAQBAJ>
- [28] P. Legg, "Use of mmwave technology for backhaul, fronthaul and access networks," 5GPPP and European Commission, Brussels, Belgium, Rep. H2020-ICT-2014-2 671551, Oct. 2017.
- [29] H. Assasa, "Robust and reliable millimeter wave wireless networks," Ph.D. dissertation, Dept. Telematic Eng., Universidad Carlos III de Madrid, Madrid, Spain, 2019.
- [30] L. L. Peterson and B. S. Davie, "End-to-end protocols," in *Computer Networks* (The Morgan Kaufmann Series in Networking), L. L. Peterson and B. S. Davie, Eds. Boston, MA, USA: Morgan Kaufmann, 2012, pp. 391–476. [Online]. Available: <http://www.sciencedirect.com/science/article/pii/B9780123850591000053>
- [31] E. J. Anderson and R. R. Weber, "The rendezvous problem on discrete locations," *J. Appl. Probab.*, vol. 27, no. 4, pp. 839–851, 1990.
- [32] O. J. Woodman, "An introduction to inertial navigation," Comput. Lab., Univ. Cambridge, Cambridge, U.K., Rep. UCAM-CL-TR-696, 2007.
- [33] T. Nescher and A. Kunz, "Analysis of short term path prediction of human locomotion for augmented and virtual reality applications," in *Proc. Int. Conf. Cyberworlds*, 2012, pp. 15–22.
- [34] J. B. Kuipers, *Quaternions and Rotation Sequences: A Primer With Applications to Orbits, Aerospace and Virtual Reality*. Princeton, NJ, USA: Princeton Univ., 1999. [Online]. Available: <https://cds.cern.ch/record/710564>
- [35] S. O. H. Madgwick, A. J. L. Harrison, and R. Vaidyanathan, "Estimation of IMU and MARG orientation using a gradient descent algorithm," in *Proc. IEEE Int. Conf. Rehabil. Robot.*, Jun. 2011, pp. 1945–1901.



**Zaheer Khan** received the Dr.Sc. degree in electrical engineering from the University of Oulu, Finland, and the M.Sc. degree in electrical engineering from University College Borås, Sweden, in 2011 and 2007, respectively. He is currently an Adjunct Professor with the University of Oulu, Finland. He has also worked for a Tenure Track Lecturer position with the University of Liverpool, U.K. from 2016 to 2017, and as a Research Fellow/Principal Investigator with the University of Oulu from 2011 to 2016. His research interests include implementa-

tion of advanced signal processing and wireless communications algorithms on Xilinx FPGAs and Zynq System-on-Chip boards, application of game theory to model distributed wireless networks, prototyping access protocols for wireless networks, IoT location tracking systems, machine learning for wireless communications design, and wireless signal design. He was a recipient of the Marie Curie Fellowship for 2007–2008.



**Janne J. Lehtomäki** (Member, IEEE) received the Doctorate degree from the University of Oulu, Finland, in 2005. He is currently an Adjunct Professor with the Center for Wireless Communications, University of Oulu. He spent the fall 2013 semester with the Georgia Tech, Atlanta, GA, USA, as a Visiting Scholar. He is currently focusing on spectrum measurements and terahertz band wireless communication. He has coauthored the paper receiving the Best Paper Award in IEEE WCNC 2012. He has served as a Guest Associate

Editor for the *IEICE Transactions on Communications* Special Section (February 2014 and July 2017) and as a Managing Guest Editor for *Nano Communication Networks* Special Issue (June 2016). He was the General Co-Chair of IEEE WCNC 2017 International Workshop on Smart Spectrum, the TPC Co-Chair for IEEE WCNC 2015 and 2016 International Workshop on Smart Spectrum, publicity/publications co-chair for ACM NANOCOM 2015, 2016, and 2017. He is the Editorial Board Member of *Physical Communication*.



**Valerio Selis** was born in Cagliari, Sardinia, Italy, in 1983. He received the Ph.D. degree in electrical engineering and electronics from the University of Liverpool, Liverpool, U.K. He is currently working as a Lecturer with the Advanced Networks Research Group, University of Liverpool. His recent research was focused on the "Adaptive Communications Transmission Interface" Project in collaboration with Queen's University Belfast, Plextek Ltd., and the Defence, Science, and Technology Laboratory. He has been the Product Development Director with

Traffic Observation via Management Ltd. His research interests include trust management, Internet of Things, embedded systems, machine-to-machine communications, wireless networks, network security, and nano-communication networks.



**Hamed Ahmadi** received the Ph.D. degree from the National University of Singapore in 2012, where he was a Ph.D. Scholar with the Institute for Infocomm Research, A-STAR. Since then, he worked at different academic and industrial positions in Republic of Ireland and U.K. He is an Assistant Professor with the Department of Electronic Engineering, University of York, U.K. He is also an Adjunct Assistant Professor with the School of Electrical and Electronic Engineering, University College Dublin, Ireland. He has published more than 60 peer

reviewed book chapters, journal, and conference papers. His current research interests include design, analysis, and optimization of wireless communications networks, the application of machine learning in wireless networks, airborne networks, blockchain, Internet-of-Things, cognitive radio networks, and small cell and self-organizing networks.



**Alan Marshall** (Senior Member, IEEE) holds the Chair in Communications Networks with the University of Liverpool, where he is the Director of the Advanced Networks Group and Head of the Department. He is a Fellow of the Institution of Engineering and Technology. He has spent over 24 years working in the Telecommunications and Defense Industries. He has been a Visiting Professor in network security with the University of Nice/CNRS, France, and an Adjunct Professor for Research with Sunway University Malaysia. He has

published over 200 scientific papers and holds a number of joint patents in the areas of communications and network security. He has formed a successful spin-out company Traffic Observation and Management Ltd. His research interests include network architectures and protocols, mobile and wireless networks, network security, high-speed packet switching, QoS/QoE architectures, and multi-sensory communications, including haptics and olfaction.